

Satellite Dynamics About Tri-Axial Ellipsoids

D.J. Scheeres
Jet Propulsion Laboratory
California Institute of Technology
Pasadena, CA

Abstract

Current planning for the Near Earth Asteroid Rendezvous (NEAR) mission includes an orbital phase about an asteroid. The current mission design stipulates Eros as the target asteroid. For science purposes it is desired to orbit the asteroid as closely and as safely as possible for an extended period of time (100+ days). However, due to the extremely distorted shape of Eros ($\approx 40 \times 14 \times 14$ km), satellite orbits are significantly non-Keplerian and include, among others, crashing, escaping and stable orbits, all starting with local circular velocity and zero eccentricity.

This example introduces the problems associated with modeling orbiters about small bodies which are significantly non-spheroid. For pre-mission planning purposes it is desired to derive qualitatively accurate scenarios of the orbital phase when the only available information pertaining to such bodies may be their major dimensions, rotation rate and rotation pole.

We propose to model these bodies as constant density, uniformly rotating tri-axial ellipsoids. The potential field of such a body and its gradients may be computed using the classical result of Ivory's theorem. Given this system, it is possible to discuss a variety of interesting classes of orbits about the body. First general results on synchronous, circular orbits about a rotating ellipsoid are discussed. Then, for a few specific asteroid models, families of planar and out-of-plane periodic orbits are computed. Finally, possible simplifications to the general dynamical system are investigated by describing the tri-axial ellipsoid in terms of a J_2 parameter. This provides simple analytic expressions for the secular variation of a satellite's orbital elements. It is noted that these secular variations can be quite large, leading to satellite motion which is significantly non-Keplerian.

We believe that the study of satellite motion about tri-axial ellipsoids is a significant topic. First, as many planned space-science missions will be orbiting small bodies with non-spheroid shapes. Second, as this is a non-trivial, non-integrable open problem in astrodynamics. This paper will serve as an introduction to this problem and present some basic results and methods of study for this problem.

1 Introduction

Mission plans are being made which visit and orbit spacecraft about various asteroids and other small bodies, such as comets. Due to the small size of most asteroids, their shape tends to differ markedly from the spheroid shapes found for all the planets of the Solar system and most of their moons. Resulting from this geometric difference, satellite dynamics about small bodies tend to be quite different, than "classical" orbiter missions. This paper introduces the tri-axial ellipsoid, a well-known and easily specified model, as a basic model for a small body gravitational field. The fundamentals of satellite dynamics about a general ellipsoid are studied. These include zero velocity surfaces, synchronous orbits, periodic orbits and analytic approximations. Also, a classification scheme is introduced for ellipsoids, dependent on the stability of certain orbits about the body.

2 Model Specification and Derivation

The tri-axial ellipsoid model of a small body is easily specified once the size, shape, density and rotation rate of a small body is given. All these quantities may be estimated or inferred, to some degree of accuracy, from ground-based measurements. The ellipsoid model would not be used in operational scenarios, as spherical harmonics are preferred in that context, but is very useful in characterizing the qualitative dynamics which satellites will encounter at asteroids or other irregularly shaped bodies.

2.1 Physical Characteristics

If the size and shape of a small body is determined (via brightness magnitudes and their variations and/or occultations), the resulting dimensions of that body are usually given in terms of "bread-box" dimensions, i.e. they specify the size of the bread-box which would contain the body. The actual shape and small scale characteristics usually cannot be determined until optical or radar imaging of the body is obtained. Given this ambiguity, there are a wide range of possible shapes the body may have. Suppositions range from ellipsoidal shapes to dumbbell shapes. The tri-axial ellipsoid (or the ellipsoid) is a useful model as it has a wide range of possible shapes generated by adjusting the shape parameters. Varying these, the body may be deformed from a sphere to a cigar to a pancake. The ellipsoid is simple to specify geometrically, all one needs are the three major axes. Given a constant density for the asteroid and its shape and size, there are classical formulae for the gravitational potential and its first and second partials. These formulae all entail evaluating elliptic integrals, for which simple and robust numerical procedures exist.

If the bread-box size measurements of a body are $a \times b \times c$, where $a \geq b \geq c$, then the associated tri-axial ellipsoid has major semi-axes of $a/2 \times b/2 \times c/2$. Let $\alpha = a/2$, $\beta = b/2$ and $\gamma = c/2$. Then the ellipsoid is specified by its major semi-axes $\alpha \times \beta \times \gamma$, where $\alpha \geq \beta \geq \gamma$.

Given a constant density ρ for the body, its gravitational parameter μ is computed as:

$$\mu = \frac{4\pi}{3} G \rho \alpha \beta \gamma \quad (1)$$

where G is the gravitational constant and $\frac{4\pi}{3} \alpha \beta \gamma$ is the volume of the ellipsoid.

Now define a body-fixed coordinate system in the ellipsoid. The x axis lies along the largest dimension α , the y axis lies along its intermediate dimension β and the z axis lies along its smallest dimension γ .

This analysis assumes that the ellipsoid rotates uniformly about its largest moment of inertia, thus the ellipsoid rotates uniformly about the z axis. The rotation rate of the ellipsoid is denoted as ω and may be inferred from ground measurements. It is possible to generalize this model to an ellipsoid with nutation and precession, but this is not performed in this analysis,

2.2 Gravitational Potential

The gravitational potential corresponding to a constant density tri-axial ellipsoid is classically known as a function of elliptic integrals. There are two forms of the potential, dependent on whether the point in question is in the interior of the ellipsoid or lies exterior to the ellipsoid.

If in the interior of the ellipsoid, the gravitational potential at a point x, y, z is (Reference MacMillan):

$$V(x, y, z) = \frac{3\mu}{4} \int_0^\infty \phi(x, y, z; u) \frac{du}{\Delta(u)} \quad (2)$$

$$\phi(x, y, z; u) = \left[\frac{x^2}{\alpha^2 + u} + \frac{y^2}{\beta^2 + u} + \frac{z^2}{\gamma^2 + u} - 1 \right] \quad (3)$$

$$\Delta(u) = \sqrt{(\alpha^2 + u)(\beta^2 + u)(\gamma^2 + u)} \quad (4)$$

Note that $V \leq 0$ always.

The generalization of this potential to the exterior of the ellipsoid is performed using Ivory's theorem. See MacMillan for a derivation of this result. Then the gravitational potential of an ellipsoid at a point x, y, z exterior to the body is:

$$V(x, y, z) = \frac{3\mu}{4} \int_{\lambda(x,y,z)}^{\infty} \phi(x, y, z; u) \frac{du}{\Delta(u)} \quad (5)$$

$$\phi(x, y, z; \lambda(x, y, z)) = 0 \quad (6)$$

where ϕ and Δ are defined as before. The parameter λ is a function of x, y, z and is solved for implicitly from Equation 6 and defines the ellipsoid passing through the point x, y, z which is confocal to the body's ellipsoid, Equation 6 is a cubic equation in λ and has a unique positive root λ whenever

$$\phi(x, y, z; 0) > 0 \quad (7)$$

(when x, y, z lies outside the ellipsoid), has the root $\lambda = 0$ when $\phi(x, y, z; 0) = 0$ (when x, y, z lie on the ellipsoid surface), and is not needed in the interior of the ellipsoid (when $\phi(x, y, z; 0) < 0$). Thus the potential defined by Equation 5 is valid for the exterior and interior of the ellipsoid as long as $\lambda \equiv 0$ whenever in the interior of the ellipsoid.

It is important to note that the potential is only twice differentiable over the entire space, there being a discontinuity in the second partials when passing from the exterior to the interior of the ellipsoid, or vice-versa (Reference MacMillan). This is immediately understood when noting that the potential solves Laplace's equation $\nabla^2 V = 0$ outside the body and Poisson's equation $\nabla^2 V = 4\pi$ inside the body. Despite this, trajectories which pass from exterior to interior or vice-versa are well defined and conserve the existing integrals of motion.

3 Equations of Motion

The equations of motion of a particle attracted by an ellipsoid can be written as:

$$\ddot{\tilde{x}} = -V_{\tilde{x}} \quad (8)$$

$$\ddot{\tilde{y}} = -V_{\tilde{y}} \quad (9)$$

$$\ddot{\tilde{z}} = -V_{\tilde{z}} \quad (10)$$

where the coordinates $\tilde{x}, \tilde{y}, \tilde{z}$ are referenced to an inertial frame.

Note that a transformation to the body fixed coordinates must be made to evaluate the partials of V . To alleviate this cumbersome transformation, transform the equations of motion into a coordinate frame rotating at the same uniform rate, ω , as the ellipsoid. This results in the equations of motion:

$$\ddot{x} - 2\omega\dot{y} = \omega^2 x - V_x \quad (11)$$

$$\ddot{y} + 2\omega\dot{x} = \omega^2 y - V_y \quad (12)$$

$$\ddot{z} = -V_z \quad (13)$$

The full partial for V_x is computed explicitly as:

$$V_x(x, y, z) = \frac{3\mu}{4} \int_{\lambda(x,y,z)}^{\infty} \phi_x(x, y, z; u) \frac{du}{\Delta(u)} - \frac{3\mu}{4} \phi(x, y, z; \lambda) \frac{\lambda_x}{\Delta(\lambda)} \quad (14)$$

Note, however, that $\phi(x, y, z; \lambda) \equiv 0$ by definition, yielding a simplified expression

$$V_x(x, y, z) = \frac{3\mu}{4} \int_{\lambda(x,y,z)}^{\infty} \phi_x(x, y, z; u) \frac{du}{\Delta(u)} \quad (15)$$

with similar formulae for the other first partials.

It is immediately clear that there is a Jacobi integral for these equations:

$$\frac{1}{2}(\dot{x}^2 + \dot{y}^2 + \dot{z}^2) - \frac{1}{2}\omega^2(x^2 + y^2) + V(x, y, z) = -C. \quad (16)$$

The parameter C is a constant and is termed the "energy" of the system

4 Normalization of the Equations of Motion

To give the discussion clarity and generalization, it is useful to normalize the equations of motion via a time and length scale. Denote the scale time to be $1/\omega$ and the non-dimensional time as τ :

$$\tau = \omega t. \quad (17)$$

Choose the largest semi-axis of the ellipsoid, α , to be the length scale and the non-dimensional space variables to be \hat{x} , \hat{y} and \hat{z} where

$$\hat{x} = x/\alpha \quad (18)$$

$$\hat{y} = y/\alpha \quad (19)$$

$$\hat{z} = z/\alpha. \quad (20)$$

Applying the normalizations to the equations of motion yields:

$$\ddot{\hat{x}} - 2\dot{\hat{y}} = \hat{x} - \hat{V}_{\hat{x}} \quad (21)$$

$$\ddot{\hat{y}} + 2\dot{\hat{x}} = \hat{y} - \hat{V}_{\hat{y}} \quad (22)$$

$$\ddot{\hat{z}} = -\hat{V}_{\hat{z}}. \quad (23)$$

The potential V is now defined as:

$$\hat{V} = \frac{\mu}{\omega^2 \alpha^3} \frac{3}{4} \int_{\lambda}^{\infty} \phi(\hat{x}, \hat{y}, \hat{z}; v) \frac{dv}{\Delta(v)} \quad (24)$$

$$\Delta(v) = \sqrt{(1+v)(\hat{\beta}^2 + v)(\hat{\gamma}^2 + v)} \quad (25)$$

$$\phi(\hat{x}, \hat{y}, \hat{z}; \lambda) = \frac{\hat{x}^2}{1+\lambda} + \frac{\hat{y}^2}{\hat{\beta}^2 + \lambda} + \frac{\hat{z}^2}{\hat{\gamma}^2 + \lambda} - 1 \quad (26)$$

$$\hat{\beta} = \beta/\alpha \quad (27)$$

$$\hat{\gamma} = \gamma/\alpha. \quad (28)$$

The parameter $\lambda > 0$ is solved for from $\phi(\hat{x}, \hat{y}, \hat{z}; \lambda) \equiv 0$ whenever $\phi(\hat{x}, \hat{y}, \hat{z}; 0) > 0$, else $\lambda = 0$.

The ratio $\delta = \mu/(\omega^2 \alpha^3)$ parameterizes the ellipsoid and is a function of the ellipsoid shape, size, density and rotation rate. Note that these are all quantities which may be inferred, to some degree of accuracy, from Earth based observations. The parameter δ is, effectively, the ratio of the gravitational acceleration to the centripetal acceleration acting on a particle at the longest end of the ellipsoid, assuming that the ellipsoid has all its mass concentrated at the origin. Should the ellipsoid be a sphere, then it is the true gravitational acceleration to centripetal acceleration ratio on the equator. See Appendix A for a listing of this parameter for some known asteroids. Note that the density of asteroids and comets is a poorly known quantity in general, thus we have assumed some nominal values in the following analysis.

Given the shape, size and rotation rate of an ellipsoid, there is a minimum δ for the body to be physically feasible. Should the density of the body be too small, or the rotation rate be too large, then the body may not be able to hold particles on its surface by gravitational attraction

alone. In this context, a limit on δ may be related to a minimum density for the body to hold itself together gravitationally. This question is discussed later in the context of synchronous orbits.

It is also possible to normalize the potential \hat{V} so that it is analogous to a point mass. This may be performed using MacLaurin's Theorem (Reference MacMillan) which states that two confocal ellipsoids may have an equivalent exterior gravitational potential if the respective masses associated with each potential are properly scaled, or that

$$V_1(x, y, z; \alpha_1, \beta_1, \gamma_1)/M_1 = V_2(x, y, z; \alpha_2, \beta_2, \gamma_2)/M_2 \quad (29)$$

where

$$\alpha_2^2 = \alpha_1^2 + \kappa \quad (30)$$

$$\beta_2^2 = \beta_1^2 + \kappa \quad (31)$$

$$\gamma_2^2 = \gamma_1^2 + \kappa \quad (32)$$

and M_1 and M_2 are the respective masses of the ellipsoids. This normalization is not introduced into the analysis as it destroys the physical significance of the ellipsoid dimensions and leads to a more difficult evaluation of the elliptic integrals.

To state the final form of the equations, drop the hat notation, assuming all quantities to be normalized, and define a modified force potential U :

$$\ddot{x} - 2\dot{y} = U_x \quad (33)$$

$$y + 2\dot{x} = U_y \quad (34)$$

$$\ddot{z} = U_z \quad (35)$$

$$u = \frac{1}{\alpha} (x^2 + y^2) - \delta V(x, y, z) \quad (36)$$

$$V = \frac{3}{4} \int_{\lambda}^{\infty} \phi(x, y, z; v) \frac{dv}{\Delta(v)} \quad (37)$$

$$\Delta(v) = \sqrt{(1+v)(\beta^2+v)(\gamma^2+v)} \quad (38)$$

$$\phi(x, y, z; v) = \frac{x^2}{1+v} + \frac{y^2}{\beta^2+v} + \frac{z^2}{\gamma^2+v} - 1 \quad (39)$$

$$\delta = \frac{\mu}{\omega^2 \alpha^3} \quad (40)$$

The parameter $\lambda > 0$ is solved for from $\phi(x, y, z; \lambda) \equiv 0$ whenever $\phi(x, y, z; 0) > 0$, else $\lambda = 0$. Also, the inequalities $1 \geq \beta \geq \gamma$ are assumed to hold.

5 Symmetries in the Equations of Motion

There are a number of symmetries present in these equations, due to the form of the potential U . First note the three-fold symmetry of U :

$$U(x, y, z) = U(\pm x, \pm y, \pm z). \quad (41)$$

This holds as U and λ are functions of x^2, y^2 and z^2 only.

In terms of the full equations of motion, and the space and time coordinates, the equations are invariant under the transformations:

$$(x, y, z, \tau) \rightarrow (x, y, -z, \tau) \quad (42)$$

$$(x, y, z, \tau) \rightarrow (x, -y, z, -\tau) \quad (43)$$

$$(x, y, z, \tau) \rightarrow (-x, y, z, -\tau) \quad (44)$$

$$(x, y, z, \tau) \rightarrow (-x, -y, z, \tau). \quad (45)$$

All these transformations may be composed onto tack other to find additional invariant transformations.

Another way to view these transformations is as how they act on initial conditions and time. Motions starting from the following initial condition pairs can be transformed into each other under the appropriate transformations given above.

$$(x_o, y_o, z_o, \dot{x}_o, \dot{y}_o, \dot{z}_o, \tau_o) \rightarrow (x_o, y_o, -z_o, \dot{x}_o, \dot{y}_o, -\dot{z}_o, \tau_o) \quad (46)$$

$$(x_o, y_o, z_o, \dot{x}_o, \dot{y}_o, \dot{z}_o, \tau_o) \rightarrow (x_o, -y_o, z_o, -\dot{x}_o, \dot{y}_o, -\dot{z}_o, -\tau_o) \quad (47)$$

$$(x_o, y_o, z_o, \dot{x}_o, \dot{y}_o, \dot{z}_o, \tau_o) \rightarrow (-x_o, y_o, z_o, \dot{x}_o, -\dot{y}_o, -\dot{z}_o, -\tau_o) \quad (48)$$

$$(x_o, y_o, z_o, \dot{x}_o, \dot{y}_o, \dot{z}_o, \tau_o) \rightarrow (-x_o, -y_o, z_o, -\dot{x}_o, -\dot{y}_o, \dot{z}_o, \tau_o). \quad (49)$$

The reversal of the time sign indicates that the transformed motion goes backwards in time.

A special subset of these initial conditions are those which transform into themselves, leading to motion which is symmetric about a line in a plane. Should any orbit have two such symmetries, then it is a periodic orbit. These are discussed later.

6 Zero-Velocity Surfaces

The first topic of qualitative interest are the zero-velocity surfaces and their interpretation. Recall the Jacobi integral (Equation 16):

$$T' = U - C. \quad (50)$$

The quantity T' is the kinetic energy with respect to the rotating reference frame, U is the force potential (Equation 36) and C is the energy constant, defined by the satellite initial conditions. Note that, by definition, $U > 0$. Thus, if $C < 0$, then $T' > 0$ and the satellite can never come to rest in the rotating frame. Further, there are no *a priori bounds on* where the particle may not travel.

Conversely, should $C > 0$, then there is the possibility that $T' = 0$ on some surface in x, y, z space, called a surface of zero-velocity. These surfaces are important as they partition the space into regions of allowable ($T' > 0$) and unallowable ($T' < 0$) motion. Of special interest are any surfaces which guarantee that the particle is trapped in the vicinity of the ellipsoid or is bounded away from the ellipsoid.

As is the usual procedure in such analyses, first consider the zero-velocity surface when $C \gg 0$ and then discuss the changes in these surfaces as C decreases towards 0. Setting $T' = 0$, the equation to solve to find the zero-velocity surfaces is:

$$\frac{1}{2}(\dot{x}^2 + \dot{y}^2) - \delta V(x, y, z) = C. \quad (51)$$

See Figure 1 for a heuristic picture of the Zero-Velocity Surfaces as projected into the $x-y$ plane for a variety of energies,

First recall that $V(x, y, z) \leq 0$. Then note that $V(x, y, z) \geq V(0, 0, 0)$, thus if $C + \delta V(0, 0, 0) > 0$, then there is only one solution to this equation, a perturbed cylinder of radius $r = \sqrt{2C + \delta V(x, y, z)} < \sqrt{2C}$. As $C \rightarrow \infty$, or as $2 \rightarrow \pm\infty$, then $r \rightarrow \sqrt{2C}$. Motion is allowable outside of this cylinder only. As C decreases this cylinder moves inward.

When $C = -\delta V(0, 0, 0)$ another zero-velocity surface bifurcates at the center of the ellipsoid. As C decreases further this zero-velocity surface expands and, depending on the parameters of the ellipsoid, may eventually intersect and then surround the ellipsoid itself, leaving space between the zero-velocity surface and the surface of the ellipsoid. At this point, motion is allowable in the space above the surface of the ellipsoid, and such motion cannot escape from the vicinity of the ellipsoid. As before, there is still a zero-velocity surface which separates the space near the ellipsoid from the space far from the ellipsoid. Thus there is a band surrounding the ellipsoid where motion is not possible.

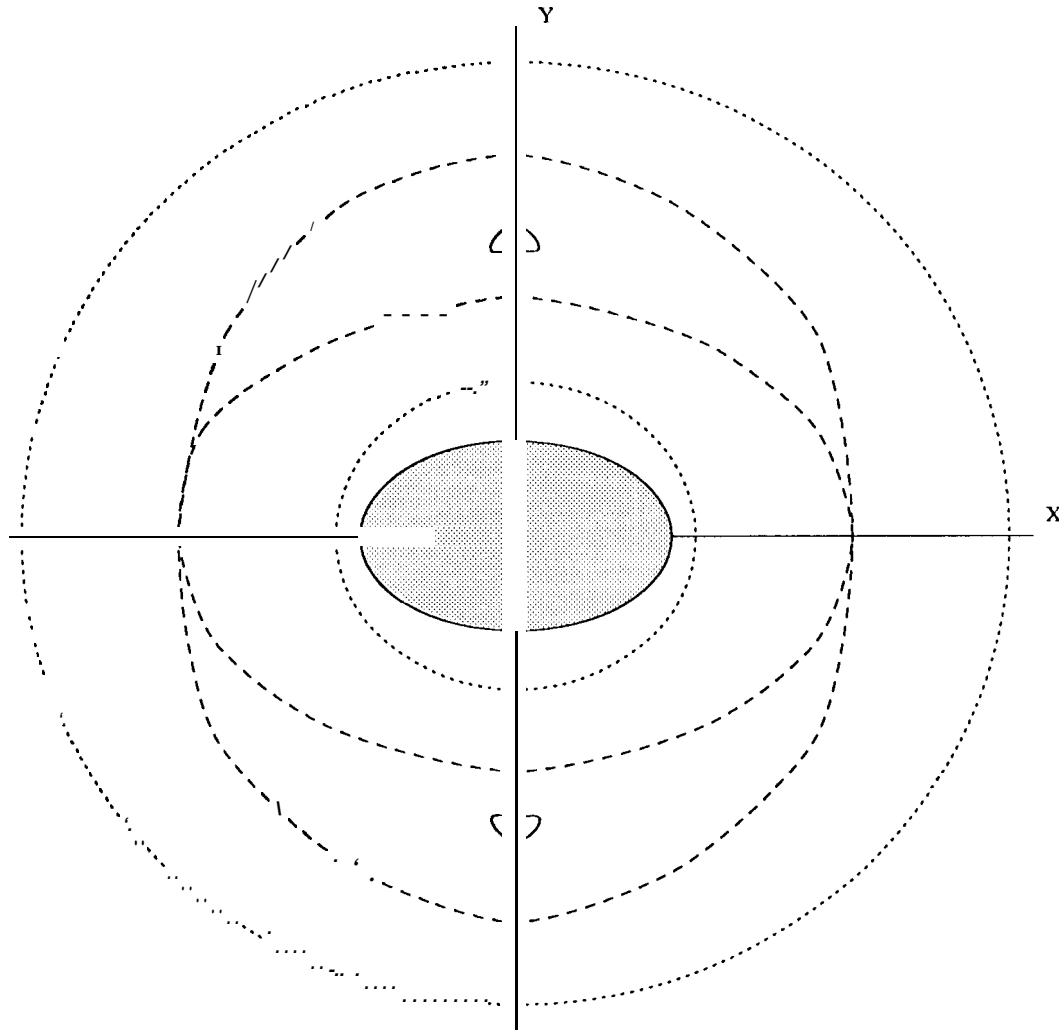


Figure 1: Zero-Velocity Curves

As the energy increases further, these two surfaces will touch at two symmetric points along the x -axis. The location of these points may be computed by solving the algebraic equation:

$$U_x(\pm x_o, 0, 0) = 0 \quad (52)$$

$$x_o \neq 0 \quad (53)$$

$$\lambda = x_o^2 - 1. \quad (54)$$

These points correspond to relative equilibrium points in the dynamical system and are discussed in Section 7. For C decreasing from this value, particles may then travel between the space close to the ellipsoid and the space far from the ellipsoid.

As the energy decreases further, the zero-velocity surfaces projected in the x - y plane shrink to two symmetric points along the y axis, found by solving the algebraic equation:

$$U_y(0, \pm y_o, 0) = 0 \quad (55)$$

$$y_o \neq 0 \quad (56)$$

$$\lambda = y_o^2 - 1. \quad (57)$$

Again, these are equilibrium points and are discussed in the following section. For decreasing C the zero-velocity surfaces then do not intersect the x - y plane and only exist in the out-of-plane space. As $C \rightarrow 0^+$, the zero-velocity surfaces shrink and move to the points $x = 0, y = 0, z = \pm\infty$, where they disappear when $C = 0$.

Note that these zero-velocity surfaces only have practical application when one considers direct orbits about the ellipsoid in inertial space. Retrograde orbits (in inertial space) generally have $T' \gg 0$ with respect to the rotating frame. 'I'bus, while they often prove to be quite stable, their energy is such that there is no zero-velocity barrier between them and the ellipsoid. This points to deficiencies in using Hill stability as a complete characterization of stability of motion.

7 Equilibrium Points

In studying direct orbits about an ellipsoid in an inertial frame, it is of interest to find circular, synchronous orbits. In the rotating reference frame, these synchronous orbits are equilibrium points of the equations of motion. For ellipsoids of revolution about the equator ($\alpha = \beta$), there are an infinity of such points. For a general tri-axial ellipsoid, there are at most four such points exterior to the body.

Algebraically, these points are found by finding all solutions to the equations:

$$U_x(x_o, y_o, z_o) = 0 \quad (58)$$

$$U_y(x_o, y_o, z_o) = 0 \quad (59)$$

$$U_z(x_o, y_o, z_o) = 0. \quad (60)$$

It is immediately apparent that $[J_z = 0$ if and only if $z = 0$. Thus the problem may be reduced to finding all solutions of

$$x_o \left[1 - \frac{3\delta}{2} \int_0^\infty \frac{dv}{(1+v)\Delta(v)} \right] = 0 \quad (61)$$

$$y_o \left[1 - \frac{3\delta}{2} \int_0^\infty \frac{dv}{(\beta^2 + v)\Delta(v)} \right] = 0 \quad (62)$$

$$\phi(x_o, y_o, 0; \lambda) = 0. \quad (63)$$

Solutions to these equations are discussed in the following subsections.

7.1 Interior Equilibrium Point

First consider the solution $x_o = y_o = 0$. This solution is well defined as the potential and the first and second partials are well defined in the interior of the ellipsoid. Recall again that $\lambda \equiv 0$ whenever inside the ellipsoid. Call this the Interior Equilibrium Point and denote its coordinates as $x_i = y_i = 0$.

7.2 Saddle Equilibrium Points

Next consider the solution when $x_o \neq 0$ and $y_o = 0$. The equation to solve in this case reduces to:

$$1 = \frac{3\delta}{2} \int_0^\infty \frac{dv}{(1+v)\Delta(v)} \quad (64)$$

$$\lambda_o = x_o^2 - 1. \quad (65)$$

Note that the solution λ_o , and hence x_o also, may be expressed in part by elliptic functions. We do not use this property explicitly, but instead solve Equation 64, when necessary, using the implicit

function theorem and Newton iteration. Call these the Saddle Equilibrium Points, for reasons which will become obvious, and denote their coordinates by $\pm x_s$ and $y_s = 0$.

It is interesting to note that these equilibrium points are not guaranteed to exist. If the inequality

$$1 < \frac{3\delta}{2} \int_0^\infty \frac{dv}{(1+v)\Delta(v)} \quad (66)$$

is violated, then the saddle equilibrium points do not exist, either interior or exterior to the ellipsoid. Note the following inequality and identity,

$$1 = \frac{3}{2} \int_0^\infty \frac{dv}{(1+v)^{5/2}} \leq \frac{3}{2} \int_0^\infty \frac{dv}{(1+v)\Delta(v)} \quad (67)$$

This implies that a necessary condition for the inequality to be violated, and for the saddle points to not exist, is $\delta < 1$.

Should Inequality 66 be violated, then it is imagined that the ellipsoid would not be physically stable as a particle placed at the end of the ellipsoid (at $x = \pm \alpha$) would fly off due to centripetal acceleration. Otherwise the body must have an internal cohesive force in addition to gravity.

This supposition may be used to derive a minimum density for a given ellipsoid shape, size and rotation rate. First evaluate the minimum δ for the saddle points to exist:

$$1 = \frac{3\delta_{\min}}{2} \int_0^\infty \frac{dv}{(1+v)\Delta(v)} \quad (68)$$

Then the minimum density is solved for as:

$$\rho_{\min} = \omega^2 \frac{3}{4\pi G \beta \gamma} \delta_{\min} \quad (69)$$

in Equation 69 the quantities β and γ are normalized, while G and ω have their original dimensions ($G = 6.672 \times 10^{-8} \text{ cm}^3/(\text{gs}^2)$).

7.3 Center Equilibrium Points

Next consider the solution for $x_o = 0$ and $y_o \neq 0$. The equations to solve for this case reduce to :

$$1 = \frac{3\delta}{2} \int_{\lambda_o}^\infty \frac{dv}{(\beta^2 + v)\Delta(v)} \quad (70)$$

$$\lambda_o = y_o^2 - \beta^2. \quad (71)$$

Again, the solution for λ_o and y_o may be expressed in part by elliptic functions. Call these equilibrium points the Center Equilibrium Points. Their coordinates are denoted as $x_c = 0$ and $\pm y_c$. They are important, for characterizing the asteroid with respect to satellite motion.

Similar to the saddle points, there are cases when these equilibrium points do not exist. A necessary condition for these points to not exist is that the saddle points not exist. We assume in general that these equilibrium points exist in the ellipsoids under consideration.

7.4 Other Possibilities

Finally, consider the solution for $x_o \neq 0$ and $y_o \neq 0$. The equations can only be satisfied in this case if $\beta = 1$, when there will be an infinity of possible equilibrium solutions all at a radius of $r = \sqrt{\lambda + 1}$. In this case there is also a new integral of motion, conservation of angular momentum about the rotation axis of the ellipsoid. The ellipsoid is then an oblate (or prolate) spheroid and is not considered here.

8 Stability of the Equilibrium Points

The stability of the equilibrium points is an item of interest, as the phase space surrounding these points may be characterized once their stability properties are known.

Stability is inferred from a study of the solutions to the variational equations about these points. In general, the variational equations are stated as:

$$\ddot{x} - 2\dot{y} = U_{xx}|_o x + U_{xy}|_o y + U_{xz}|_o z \quad (72)$$

$$\ddot{y} + 2\dot{x} = U_{yx}|_o x + U_{yy}|_o y + U_{yz}|_o z \quad (73)$$

$$\ddot{z} = U_{zx}|_o x + U_{zy}|_o y + U_{zz}|_o z. \quad (74)$$

The partials are all evaluated at the equilibrium points. It is simple to show that all the cross partials are zero at the equilibrium points, yielding the simplified set:

$$\ddot{x} - 2\dot{y} = U_{xx}|_o x \quad (75)$$

$$\ddot{y} + 2\dot{x} = U_{yy}|_o y \quad (76)$$

$$\ddot{z} = U_{zz}|_o z. \quad (77)$$

Direct computation shows that $U_{zz}|_o < 0$ for all planar points and hence all small out-of-plane oscillations about the equilibrium points are stable. Thus we concentrate on the in-plane stability of the points.

Form the characteristic equation corresponding to the variational equations to find:

$$\sigma^4 + [4 - U_{xx}|_o - U_{yy}|_o] \sigma^2 + U_{xx}|_o U_{yy}|_o = 0 \quad (78)$$

where σ is the eigenvalue of the system. Then the stability conditions for the equilibrium points may be reduced to the following conditions:

$$U_{xx}|_o U_{yy}|_o > 0 \quad (79)$$

$$4 - U_{xx}|_o - U_{yy}|_o > 0 \quad (80)$$

$$(4 - U_{xx}|_o - U_{yy}|_o)^2 - 4U_{xx}|_o U_{yy}|_o > 0. \quad (81)$$

To compute the second partials of the function V , consider the term V_{xx} explicitly:

$$V_{xx}(x, y, z) = \frac{3\mu}{4} \int_{\lambda(x, y, z)}^{\infty} \phi_{xx}(x, y, z; u) \frac{du}{\Delta(u)} - \frac{3\mu}{4} \phi_x(x, y, z; u) \Big|_{u=\lambda} \frac{\lambda_x}{\Delta(\lambda)} \quad (82)$$

Now the final term in the equation does not disappear, as it did for V_x . From the following identities:

$$\phi(x, y, z; \lambda) \equiv 0 \quad (83)$$

$$\frac{\partial \phi(x, y, z; \lambda)}{\partial x} \equiv 0 \quad (84)$$

the general expression for λ_x may be inferred:

$$\lambda_x = \frac{2x}{1 + \lambda \frac{1}{\frac{x^2}{(1+\lambda)^2} + \frac{y^2}{(\beta^2+\lambda)^2} + \frac{z^2}{(\gamma^2+\lambda)^2}}} \quad (85)$$

Similar expressions are found for λ_y and λ_z . These partials simplify at the equilibrium points. Finally, with the simple expressions:

$$\phi_x(x, y, z; u) = \frac{2x}{1 + u} \quad (86)$$

$$\phi_{xx}(x, y, z; u) = \frac{2}{1 + u}, \quad (87)$$

all the elements needed to compute V_{xx} are available. The expressions for V_{yy} and V_{zz} are computed similarly.

Now the stability of each of the equilibrium points is investigated in turn.

8.1 Interior Equilibrium Point

As $\lambda \equiv 0$ for the interior point, the partials simplify to:

$$U_{xx}|_i = 1 - \frac{3\delta}{2} \int_0^\infty \frac{du}{(1+u)\Delta(u)} \quad (88)$$

$$U_{yy}|_i = 1 - \frac{3\delta}{2} \int_0^\infty \frac{du}{(\beta^2 + u)\Delta(u)} \quad (89)$$

It is important to note that, under the assumptions stated earlier, both of these quantities are negative. If not, then the saddle and perhaps the center equilibrium points would not exist. Given that these are negative, it is obvious that the stability conditions 79- 81 are all satisfied.

There is actually something more powerful occurring in this case. Examination of the first partials in the ellipsoid interior and the second partials evaluated in the vicinity of the origin show the following equality:

$$U_x(x, y, z) = U_{xx}|_i x \quad (90)$$

with similar results for y and z . Thus, for motion in the interior of the ellipsoid, the general equations of motion are time invariant linear differential equations. Thus, the solutions obtained in the vicinity of the origin are valid throughout the entire interior region of the ellipsoid.

Under the nominal assumption that $U_{xx}|_i, U_{yy}|_i < 0$, motion in the interior of the ellipsoid is a stable, harmonic motion. It is useful to briefly investigate what the stability conditions are when the nominal assumption is violated. First note the following inequalities:

$$U_{xx}|_i \leq 1 \quad (91)$$

$$U_{yy}|_i \leq 1 \quad (92)$$

These are easily established by inspection and hold for all possible parameter values. From these inequalities it is clear that the stability conditions 80 and 81 are always satisfied. However, should $U_{xx}|_i > 0$ while $U_{yy}|_i < 0$, i.e. should the saddle points not exist but the center points exist, then all motion inside the ellipsoid is hyperbolic, and will eventually exit the interior. Note that if both the saddle and center points do not exist, $U_{xx}|_i > 0$ and $U_{yy}|_i > 0$, then the interior motion is stable and harmonic again, even though the body is not likely to exist naturally.

8.2 Saddle Equilibrium Points

Recall that the saddle points have coordinates $x_s \neq 0$ and $y_s = 0$. Substituting these values into the the second partial derivatives yields:

$$U_{xx}|_s = 1 - \frac{3\delta}{2} \int_{\lambda_s}^\infty \frac{du}{(1+u)\Delta(u)} - \frac{3\delta}{\Delta(\lambda_s)} \quad (93)$$

$$U_{yy}|_s = 1 - \frac{3\delta}{2} \int_{\lambda_s}^\infty \frac{du}{(\beta^2 + u)\Delta(u)} \quad (94)$$

Again, λ_s and x_s are solved for from the equations:

$$1 = \frac{3\delta}{2} \int_{\lambda_s}^\infty \frac{dv}{(1+v)\Delta(v)} \quad (95)$$

$$\lambda_s = x_s^2 - 1. \quad (96)$$

Simplifying the second partials yields:

$$U_{xx}|_s = \frac{3\delta}{\Delta(\lambda_s)} \quad (97)$$

$$U_{yy}|_s = 1 - \frac{3\delta}{2} \int_{\lambda_s}^\infty \frac{du}{(\beta^2 + u)\Delta(u)}, \quad (98)$$

Given that $\beta < 1$, then $U_{yy}|_s < 0$, as can be inferred from Equation 95. It is also clear that $U_{xx}|_s > 0$. Thus stability condition 79 is clearly violated while condition 81 is satisfied. The status of condition 80 is not as clear. It can be simplified to some extent, however.

First note the following identity derived in Appendix B:

$$\frac{1}{\Delta(\lambda)} = \frac{1}{2} \int_{\lambda}^{\infty} \left[\frac{1}{1+u} + \frac{1}{\beta^2+u} + \frac{1}{\gamma^2+u} \right] \frac{du}{A(u)} \quad (99)$$

This may be applied to condition 80 to find the simplified condition:

$$1 > \frac{\delta}{2} \int_{\lambda_s}^{\infty} \left[\frac{1}{1+u} + \frac{1}{\gamma^2+u} \right] \frac{du}{A(u)} \quad (100)$$

This expression may be reduced to some simpler sufficiency conditions. However, these would still entail solving for the parameter δ , and hence would not greatly simplify the evaluation of the inequality. Also, this stability condition does not change the basic instability type of the saddle points, which is hyperbolic. Thus, any satellite placed at or near these points will be influenced mostly by the hyperbolic stable and unstable manifolds, and its general motion will be to depart from the vicinity of the point.

As seen in Section 6, the saddle points are the boundary points between regions of allowable motion close to and far from the ellipsoid. Thus, motion starting close to these points will in general either be trapped near the ellipsoid or trapped away from the ellipsoid. Another way of stating this is to note that one pair of each of the point's stable and unstable manifolds lies close to the ellipsoid while the other pair lies away from the ellipsoid. Thus, when passing close to these points in phase space, the final motion of a satellite will be close to or far from the ellipsoid depending upon which pair of manifolds the satellite is influenced by.

8.3 Center Equilibrium Points

Recall that the center points have coordinates $x_c = 0$ and $y_c \neq 0$. Substituting these values into the the second partial derivatives yields:

$$U_{xx}|_c = 1 - \frac{3\delta}{2} \int_{\lambda_c}^{\infty} \frac{du}{(1+u)\Delta(u)} \quad (101)$$

$$U_{yy}|_c = 1 - \frac{3\delta}{2} \int_{\lambda_c}^{\infty} \frac{du}{(\beta^2+u)\Delta(u)} + \frac{3\delta}{\Delta(\lambda_c)} \quad (102)$$

Again, λ_c and y_c are solved for from the equations:

$$1 = \frac{3\delta}{2} \int_{\lambda_c}^{\infty} \frac{dv}{(\beta^2+v)\Delta(v)} \quad (103)$$

$$\lambda_c = y_c^2 - \beta^2. \quad (104)$$

Simplifying the second partials yields:

$$U_{xx}|_c = 1 - \frac{3\delta}{2} \int_{\lambda_c}^{\infty} \frac{du}{(1+u)\Delta(u)} \quad (105)$$

$$U_{yy}|_c = \frac{3\delta}{\Delta(\lambda_c)} \quad (106)$$

Given that $\beta < 1$, then $U_{xx}|_c > 0$, as inferred from Equation 103. It is also clear that $U_{yy}|_c > 0$. Thus stability condition 79 is clearly satisfied. The status of conditions 80 and 81 are not as clear, and may or may not be satisfied, depending on the parameters of the ellipsoid: δ, β, γ .

A few notes may be made concerning the order in which conditions 80 and 81 may be violated. Assume that the parameter δ is fixed and that the parameters β and γ will be decreased

from $\beta = \gamma = 1$ (keeping $\gamma \leq \beta$), thus deforming a sphere into an ellipsoid. Taking Equations 105 and 106 to the limit for a sphere yields

$$\lim_{\beta, \gamma \rightarrow 1} U_{xx}|_c = 0 \quad (107)$$

$$\lim_{\beta, \gamma \rightarrow 1} U_{yy}|_c = 3 \quad (108)$$

Under these limits, both condition 80 and 81 are satisfied. Given this, and that condition 79 is satisfied, it is evident that condition 81 must be violated before condition 80 may be violated when deforming a sphere into a general ellipsoid. Thus, as a body is progressively deformed from a sphere, it is stability condition 81 that delineates between whether the center points are stable or unstable. If condition 80 becomes violated subsequently, it will not have as large a qualitative effect as it will only pertain to the orientation of the stable and unstable manifolds of the center points and will not affect the instability type.

For ellipsoids where all the stability conditions are satisfied, the center points are stable in the sense that most motions started near them will oscillate about the center point indefinitely. For ellipsoids where the stability condition is not satisfied, the center points become complex unstable. Then, any motion started near the center point will eventually spiral away from the center point. As there are no isolating zero-velocity surfaces associated with the center points, the final motion may either fall onto the ellipsoid or escape from the ellipsoid.

Whether the center points are stable or unstable has a large influence on the stability of near-synchronous orbits about the ellipsoid. When the center points are stable, motion started in near synchronous orbits tend to remain bounded away from the ellipsoid, as the region of regular curves in phase space near the center points makes passage through these curves to the surface of the ellipsoid difficult. It is noted in passing that near-circular orbits about ellipsoids with stable center points seem to be well behaved in general.

The same cannot be said when the center points are unstable. Now the phase space around the center points is influenced by the unstable spiral manifolds. The generic motion under the influence of these manifolds is to spiral away from the center point. It is important to note that the spiral the satellite will follow tends to act in both the angular and radial directions. The generic motion of a satellite along these unstable manifolds seems to either crash into the ellipsoid or to suffer repeated close approaches to it. Due to the distorted shape of the ellipsoid, these close approaches may cause the satellite to gain hyperbolic speeds and escape the ellipsoid. If the motion is continued through crashes with the ellipsoid the generic final motion associated with the unstable manifold is a departure from the vicinity of the ellipsoid. Thus, near-synchronous orbits about ellipsoids with unstable center points can be characterized as being unstable in general. It is not uncommon to observe a near-synchronous, near circular orbit crash onto an ellipsoid (with unstable center points) within a matter of days.

In this paper ellipsoids with stable center equilibrium points are called Type I ellipsoids, while those with unstable center equilibrium points are called Type II ellipsoids. It is evident that the crashing problem associated with Type II ellipsoids is related to near synchronous motion about the ellipsoid. Thus, when orbiting about a Type II ellipsoid, it is in general best to avoid near synchronous orbits. An effective way of doing so is to fly in a retrograde orbit about the ellipsoid. As will be seen later, retrograde orbits are associated with stable orbital motion.

8.4 Computing Ellipsoid Type

It is of interest to characterize when an ellipsoid is of Type I (stable center points) and when it is of Type II (unstable center points). In general, this characterization is a function of the three parameters: β, γ, δ . Given these numbers for any ellipsoid, it is possible to compute Stability Condition 81 and check which category the ellipsoid falls into. This condition may be represented

as a two-dimensional surface in the three-dimensional space β, γ, δ . In general, this surface may not be defined everywhere, as there may be some combinations of β and γ which are never Type II.

This procedure of computing ellipsoid type may be simplified for some cases. First note that a sufficient condition for an ellipsoid with parameters β, γ and δ to be of Type II is that the corresponding ellipsoid with $\gamma = \beta$, with δ held constant, be of Type II. This result is not established here, but can be verified by computation. This simplifies the presentation somewhat as the two dimensional surface in the three dimensional space is now collapsed into a one dimensional surface (a line) in the two dimensional space β, δ . The ellipsoid is, in this case, an ellipsoid of revolution. It is not, however, an oblate or prolate ellipsoid, as its axis of rotation is perpendicular to the axis of symmetry. Rather it is similar to a cigar lying on a table with its rotation axis perpendicular to the table. There are simplifications to the form of the stability condition for this case.

First note the following results for the center equilibrium point, assuming that $\gamma = \beta < 1$. These results may be inferred from the results given in Appendix B.

$$U_{xx}|_c = 1 - \frac{3\delta\delta}{2\lambda_c} \int_{\lambda_c}^{\infty} \frac{du}{(1+u)\Delta(u)} \quad (109)$$

$$= 3 \left(1 - \frac{\delta}{\Delta(\lambda_c)} \right) \quad (110)$$

$$U_{yy}|_c = \frac{3\delta}{\Delta(\lambda_c)} \quad (111)$$

$$A(u) = (\beta^2 + u) \sqrt{1+u} \quad (112)$$

Additionally, it is now possible to reduce the elliptic integrals to quadratures in terms of known functions. The equation from which we solve for λ_c is still, however, transcendental.

The condition for stability (Equation 81) now reduces to:

$$1 > \frac{36\delta}{\Delta(\lambda_c)} \left(1 - \frac{\delta}{\Delta(\lambda_c)} \right) \quad (113)$$

subject to the constraint

$$1 = \frac{3\delta}{2} \int_{\lambda_c}^{\infty} \frac{du}{(\beta^2 + u)^2 \sqrt{1+u}} \quad (114)$$

$$= \frac{3\delta}{2} \left[\frac{\sqrt{1+\lambda_c}}{(1-\beta^2)(\beta^2+\lambda_c)} - \frac{1}{2(1-\beta^2)^{3/2}} \ln \frac{1+\sqrt{\frac{1-\beta^2}{1+\lambda_c}}}{1-\sqrt{\frac{1-\beta^2}{1+\lambda_c}}} \right] \quad (115)$$

The curve for this condition has been generated and is shown in Figure 2. The meaning of this curve is as follows. Given the three parameters for an ellipsoid, β, γ and δ , if the β and δ values fall into the Type II portion of the surface (lie beneath the curve), then the ellipsoid is a Type II ellipsoid (assuming that $\gamma \leq \beta$). Note that if the values fall into the Type I portion of the surface, then the ellipsoid may still be a Type II ellipsoid if $\gamma < \beta$. Finally observe that the curve does not extend all the way to $\beta = 1$, but stops at a value of $\beta \approx 0.928$. For all β greater than this value, the ellipsoid with $\beta = \gamma$ can only be of Type I.

Note that δ is a function of μ, α and w . Thus δ will decrease if the mass (or density) of the ellipsoid decreases or if the size or rotation rate increases. These effects tend to make a Type I ellipsoid into a Type II ellipsoid.

9 Periodic Orbits

Now our discussion focuses on a few families of periodic orbits computed for satellite motion about an ellipsoid. These results are all numerical and are computed for only a few specific ellipsoid

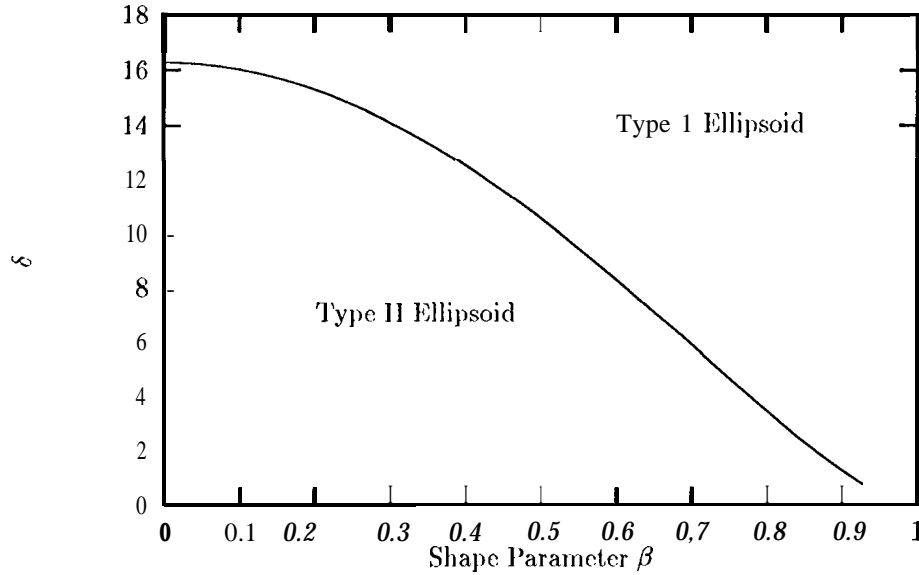


Figure 2: Minimum δ for a Type 1 ellipsoid vs β ($\gamma = \beta$)

shapes and parameters. Five planar periodic orbits are briefly discussed, three of them associated with the center and saddle equilibrium points respectively, and the remaining two being “near-circular”, one direct and the other retrograde with respect to inertial space. Finally a family of three-dimensional periodic orbits is computed and discussed.

In computing the periodic orbits, the families are either terminated once an intersection with the ellipsoid occurs or when the continued computation of the family becomes too difficult. The termination at an intersection with the ellipsoid is not necessary, as intersecting orbits are well defined and even conserve energy. The families are terminated due to some questions associated with orbit families that intersect the ellipsoid. The main question pertains to the conservation of stability properties when a family of periodic orbits intersects the ellipsoid. The question arises as there is a discontinuity in the second partials of the potential function across the ellipsoid surface. These partials are used in computing the variational equations and hence the stability of the orbits.

A way in which this problem may be avoided would be to rescale the ellipsoid to a smaller, confocal ellipsoid with a larger mass, as is detailed in MacLaurin’s Theorem (Reference MacM). For this study, this process was not pursued as the physical character of the ellipsoid is lost and as the computation of the elliptic integrals becomes more time consuming as the size of the ellipsoid is shrunk. An investigation of these questions may be of interest in future analyses.

9.1 Planar Periodic Orbits

These orbits all lie in the ellipsoid equatorial plane ($z \equiv 0$). The near-circular direct and retrograde orbits have two distinct symmetries, and thus have a quarter-symmetry in the plane similar to Hill’s famous Variation orbit. (Henon). The following pairs of boundary conditions are used to compute these orbits:

$$\begin{aligned}
 x_0 &= x_0 \\
 y_0 &= 0 \\
 \dot{x}_0 &= 0 \\
 \dot{y}_0 &= \dot{y}_0
 \end{aligned} \tag{116}$$

$$\begin{aligned}
x_1 &= 0 \\
y_1 &= y_1 \\
\dot{x}_1 &= \dot{x}_1 \\
\dot{y}_1 &= 0
\end{aligned} \tag{117}$$

Should any orbit satisfy both of these boundary conditions, then that orbit may be extended into a periodic orbit symmetric about both the x and y axes. The saddle and center periodic orbits will only satisfy one of the above symmetry conditions. In the following numerical studies we choose two basic ellipsoid to investigate, one based on the asteroid Vesta, which may be classified as a Type I asteroid, and the other based on the asteroid Eros, which may be classified as a Type II asteroid.

The stability computations of the periodic orbits follow well established procedures for planar periodic orbits (Hénon). The actual method used is described in Scheeres. They involve computation of a characteristic quantity a which must satisfy the condition $|a| < 1$ for the orbit to be stable. A similar quantity may be computed which describes the out-of-plane stability of the orbit.

9.1.1 Vesta

There are five basic families of periodic orbits about a Type I ellipsoid such as Vesta. These are the direct and retrograde orbits which have a double symmetry property, and the periodic orbits associated with the saddle and center equilibrium points, which have a single symmetry property. Additionally, there are the four equilibrium points surrounding the ellipsoid.

See Appendix A for a list of the physical properties of the asteroid Vesta. The normalized quantities are used for the following computations. The saddle equilibrium points are located at:

$$x_s = \pm 1.94097 \tag{118}$$

$$C_s = 5.565129 \tag{119}$$

The center equilibrium points are located at:

$$y_c = \pm 1.92377 \tag{120}$$

$$C_c = 5.531994 \tag{121}$$

The saddle periodic orbits are unstable, similar to the Hill problem (Hénon). The center periodic orbits are stable in general. There are two families of these orbits associated with each center equilibrium point. Analogous to the periodic orbits associated with the triangle equilibrium point, in the Restricted 3-Body Problem, these two families may be distinguished as a long period family and as a short period family. In our presentations we show only the short period family.

As expected, the family of retrograde periodic orbits are all stable. Note that the family of direct orbits at Vesta are also stable, except for some small regions of marginal stability or small instability. This strengthens the assertions of the previous section regarding Type I ellipsoids, as it is clearly possible for a satellite to follow a stable, direct orbit at fairly low altitudes. There also exists a family of stable direct orbits which lie, in the most part, at a lower altitude than the equilibrium points. This family has not been investigated for this presentation.

Figure 3 shows the periodic orbit families as lines in the x_0, C space, where x_0 is the initial coordinate along the x -axis and C is the energy of the orbit. From these two pieces of information the periodic orbit may be constructed, as the energy C may be translated into an initial velocity \dot{y}_0 which is perpendicular to the x -axis. This plot shows the direct, retrograde and saddle periodic orbit families. The center periodic orbit family is also shown, with its initial y_0 coordinate plotted

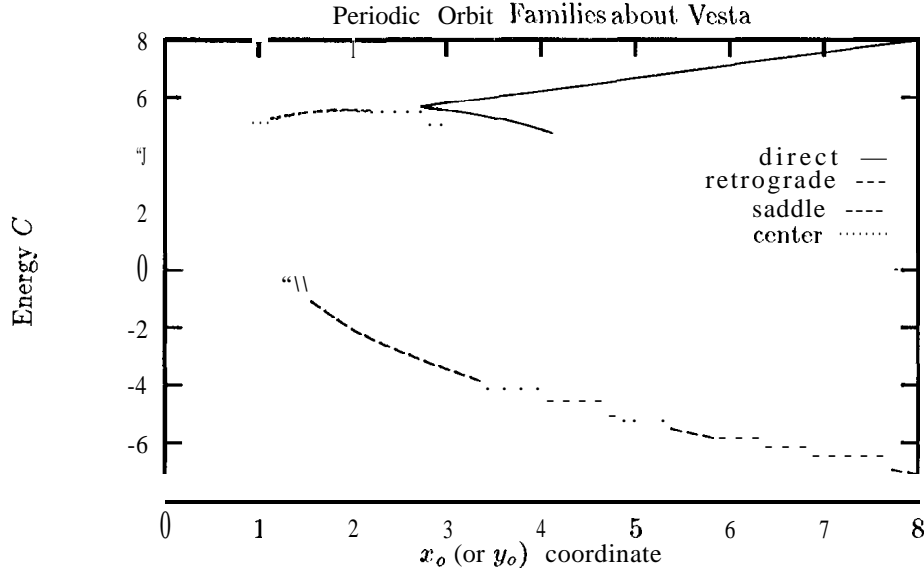


Figure 3: Periodic Orbit Families About Vesta

along the x-axis. Note that with this plotting convention, the saddle and center periodic orbit families lie very close to one another.

Figure 4 shows samples of a direct, retrograde, saddle and center periodic orbits. Note that the direct, retrograde and center periodic orbits in this plot are stable. The saddle periodic orbit is unstable. Also shown are two of the equilibrium points. Note that the saddle and center orbits and points have associated mirror images located on the other side of the asteroid. These are not shown in the figure.

9.1.2 Eros

The ellipsoid based on the asteroid Eros is a Type II ellipsoid. For a Type II ellipsoid there are only three basic families of periodic orbits. For these bodies the center points no longer generate periodic orbits in their vicinity. This is due to the local nature of the phase space about these equilibrium points, as closed orbits cannot be constructed in the linear system close to the center points.

The parameters used for the ellipsoid based on Eros are also listed in Appendix A. Note that, for convenience, the density was chosen so that $\delta = 1$. The normalized quantities are used for the following computations. The saddle equilibrium points are located at:

$$x_s = \pm 1.1926 \quad (122)$$

$$C_s = 1.6965 \quad (123)$$

The center equilibrium points are located at:

$$y_c = \pm 0.92689 \quad (124)$$

$$C_c = 1.42333 \quad (125)$$

The presentation of the direct, retrograde and saddle periodic orbit families for the ellipsoid based on Eros are shown in Figure 5. The definitions and interpretations of these orbits remain as before. There are some differences for these families, however. First, as mentioned before, there are no periodic orbit families which begin at the center equilibrium points. This is due to the complex

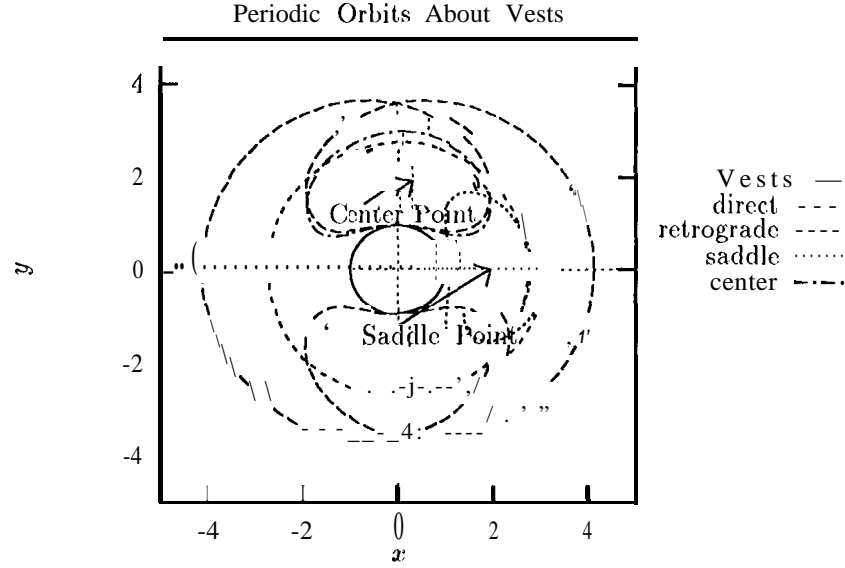


Figure 4: Sample Periodic Orbits About Vesta

unstable nature of these points, as it becomes impossible to construct a closed orbit in the immediate region of the phase space surrounding the equilibrium point. Also note that the direct orbits become unstable at a distance of 1.85 normalized units from the long end of the ellipsoid (at a radius of 37 km), and remains so for the remainder of the family, except for the small regions where the family curve passes through an extremum with respect to the energy C . Again, this highlights the danger of orbiting a Type II ellipsoid in a direct orbit within this distance as the unstable manifold of these orbits tend to intersect the ellipsoid. Conversely, as might be expected, the retrograde orbits are stable throughout the family. Thus these may be considered to be "safe" orbits in which to fly close to such an asteroid.

Not discernable from Figure 5 is that the line defining the direct family of periodic orbits terminates as a spiral in the (x_0, C) plane. The stability parameter a seemingly becomes arbitrarily large as the family is continued along this curve, although this is still an open matter. Also note the relatively larger separation between the saddle family and the direct family in Figure 5. Compare this to the family given for Vests in Figure 3.

in Figure 6 are some samples of periodic orbits about the ellipsoid based on Eros. In this plot the direct and saddle orbits are unstable while the retrograde orbit is stable.

9.2 Three-Dimensional Orbits

Next a family of out-of-plane periodic orbits is computed for the Eros based Type II ellipsoid. This family is synchronous with the rotating ellipsoid in that it only views one side of the ellipsoid as the orbit is traversed. The family is generated mainly from one symmetry boundary condition,

$$\begin{aligned}
 x_0 &= 0 \\
 y_0 &= y_0 \\
 z_0 &= 0 \\
 \dot{x}_0 &= \dot{x}_0 \\
 \dot{y}_0 &= 0 \\
 \dot{z}_0 &= \dot{z}_0
 \end{aligned}
 \tag{126}$$

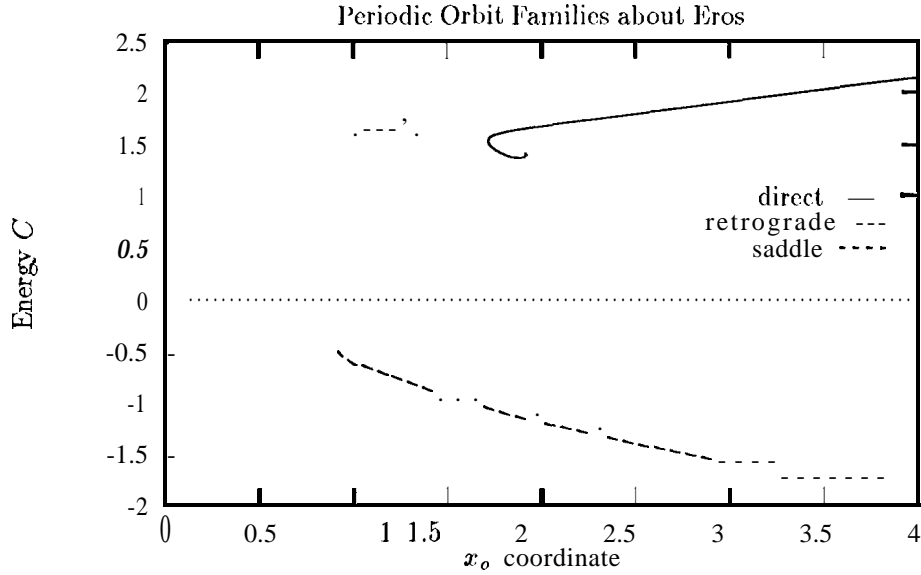


Figure 5: Periodic Orbit Families About Eros

although one of the members of the family has two distinct symmetry boundary conditions, the second condition being

$$\begin{aligned}
 x_0 &= 0 \\
 y_0 &= y_0 \\
 z_0 &= z_0 \\
 \dot{x}_0 &= \dot{x}_0 \\
 \dot{y}_0 &= 0 \\
 \dot{z}_0 &= 0.
 \end{aligned} \tag{127}$$

These symmetry boundary conditions are found by compounding the previously stated initial conditions given in Section 5.

For the computation of these orbits, a total of six boundary conditions must be met. In general, three of them are met by specifying the initial conditions: $x_0 = 0$, $z_0 = 0$, $\dot{y}_0 = 0$. The fourth boundary condition is met by proper choice of the Poincaré map surface: $z_1 = 0$. This leaves the two boundary conditions $x_1 = 0$ and $\dot{y}_1 = 0$. To achieve these boundary conditions, we may vary three parameters, the initial conditions: y_0 , \dot{x}_0 , \dot{z}_0 . Denote the general solution for the Poincaré map as:

$$x_1 = g(x_0, \dot{x}_0, \dot{z}_0) \tag{128}$$

$$\dot{y}_1 = h(x_0, \dot{x}_0, \dot{z}_0) \tag{129}$$

The remaining variables $y_1, \dot{x}_1, \dot{z}_1$ are free. Thus, computing the periodic orbit is equivalent to solving the equations:

$$0 = g(x_0, \dot{x}_0, \dot{z}_0) \tag{130}$$

$$0 = h(x_0, \dot{x}_0, \dot{z}_0) \tag{131}$$

Thus it is evident that the family of these three-dimensional periodic orbits may be described as a line in the three-dimensional initial condition space: $y_0, \dot{x}_0, \dot{z}_0$. Note that one of these initial variables may be replaced by the energy C .

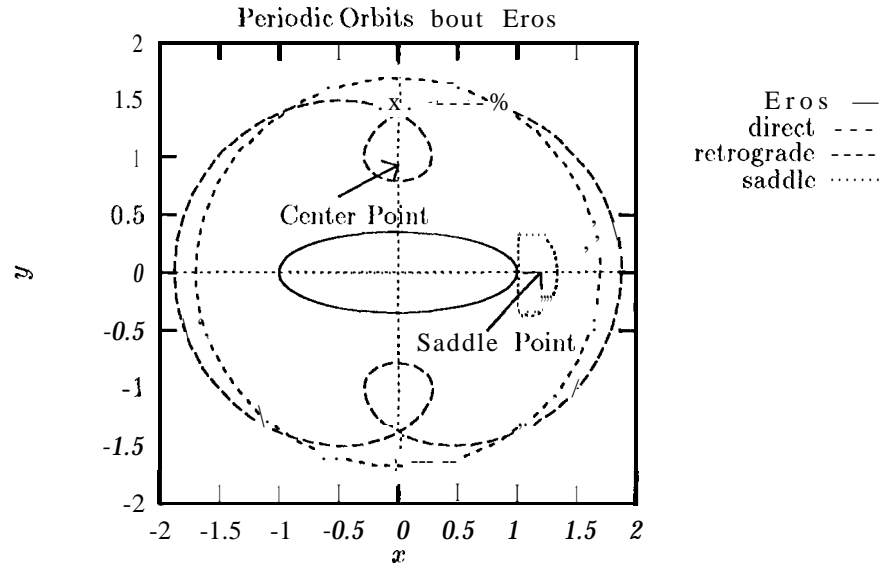


Figure 6: Sample Periodic Orbits About Eros

Select members of this family are presented in Figures 7-9. The three-dimensional orbits have been projected into the three planes: $x \times y$, $y \times z$, $z \times x$. Note that only the portion of the orbits with $z \geq 0$ have been plotted. Also note that the periodic orbit with double symmetry is denoted by the solid line in the Figures.

Finally, in Figure 10 is a three-dimensional representation of the doubly symmetric orbit and in Figure 11 is a three-dimensional representation of the periodic orbit which intersects the ellipsoid. In both plots the ellipsoid is drawn in the foreground. Thus the orbits are behind the ellipsoid, from our perspective.

The three-dimensional family is traced from intersection with the ellipsoid to an intersection of the family with a three-dimensional orbit with a double symmetry. This double symmetry family may be continued, although it appears that the topology of this family is complicated and not conducive to the usual methods of continuing families of orbits.

The orbits may be associated with the center equilibrium points as they lie close to them in the plane. Note that the double symmetry orbit intersects the y -axis in the close vicinity of the center equilibrium point. The orbit intersects the axis at $y = 0.9221$ while the center equilibrium point is at $y = .9269$. The energy of this double symmetric orbit is $C = 0.7752$, which compares with the energy $C_c = 1.4233$ for the center equilibrium point. Furthermore, if the family of doubly symmetric periodic orbits is continued, at some point they cross through the center equilibrium point coordinates on the y -axis. The relation between the center equilibrium points and these three-dimensional orbits are not fully understood and will be a topic of interest for future study.

All members of this family are unstable. The stability parameters of these orbits are computed following the description in Reference Marchal. While the problem discussed there is different, the basic stability conditions may be reduced to a similar formulation. As mentioned, for all the members of the family, the orbits are highly unstable.

10 Analytic Approximations for Non-Synchronous Motion

Finally some simple approximations are discussed which may be introduced to this problem. This approximation assumes that the satellite orbit is not near-synchronous with the ellipsoid rotation

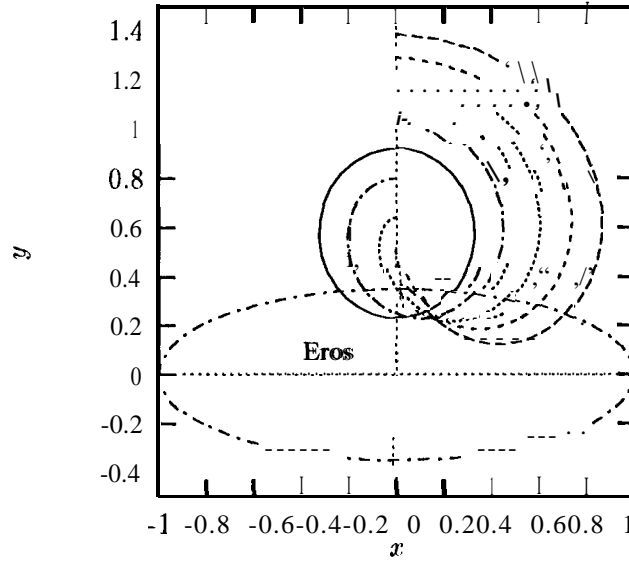


Figure 7: $x \times y$ Projection of Periodic Orbits

rate, and then replaces the ellipsoid with an equivalent oblate body. This approximation is seen to work rather well when the satellite is in a retrograde orbit about the ellipsoid, although there are some fundamental limits to the applicability of the analysis.

10.1 Derivation of a Simplified Force Potential

Restate the gravitational potential for the ellipsoid in spherical coordinates, assuming that the potential has been expanded to the second order in the inertial integrals:

$$V = \frac{-\mu}{r} \left[1 - \frac{1}{20r^2} (\alpha^2 + \beta^2 - 2\gamma^2) (3 \sin^2 \theta - 1) + 3 (\alpha^2 - \beta^2) \cos^2 \theta \cos 2(\omega t - \phi) - \dots \right] \quad (132)$$

where θ is the declination angle measured from the ellipsoid equator and ϕ is the right ascension angle measured from the x -axis.

Now introduce a particular assumption, that the satellite is not near synchronous with the ellipsoid, or $|\omega - \dot{\phi}| \gg 0$. This assumption is valid if the satellite is in a near circular orbit far from the body, or if the satellite is in a retrograde orbit with respect to the ellipsoid rotation pole. Further, in each of these cases it will be approximately true that $\phi = \dot{\phi}t$, over short intervals of time at least. Under these assumptions it is reasonable to replace the potential in Equation 132 with the potential averaged in time over one revolution of the ellipsoid, or some other appropriate scale time:

$$\bar{V} = \frac{1}{T} \int_0^T V(t) dt \quad (133)$$

Perform the averaging and note that the quantity J_2 may be identified as:

$$J_2 = \frac{1}{10} (\alpha^2 + \beta^2 - 2\gamma^2) \quad (134)$$

This definition of J_2 has dimensions of length squared, often this parameter is normalized by dividing by the largest dimension of the ellipsoid squared. Performing the averaging and making

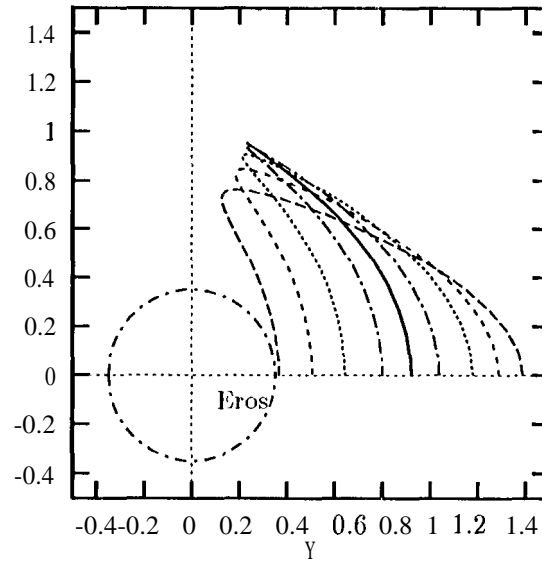


Figure 8: y x 2 Projection of Periodic. Orbits

the replacements yields the result:

$$V = \frac{-\mu}{r} \left[1 - \frac{J_2}{2r^2} (3 \sin^2 \theta - 1) + \dots \right] \quad (135)$$

Thus the ellipsoid is replaced by an equivalent oblate spheroid of the same mass, with the primary perturbation term being the J_2 term. Note that this is similar to replacing the tri-axial ellipsoid with the ellipsoid of revolution with $a = \beta$, while keeping the parameter δ constant.

While admittedly a simple approximation, it nonetheless proves to be accurate enough in many cases to serve as an appropriate design model for pre-mission planning for missions to small bodies.

10.2 Secular Changes in the Orbital Elements

Given the canonical form of the potential in Equation 135, a wealth of information exists pertaining to satellite orbits about such a body. The results of immediate interest are the secular rates of change of the orbital elements of a satellite orbiting the ellipsoid. Denote the usual orbital elements as: a , the semi-major axis; e , the eccentricity; i , the inclination; w , the argument of the periapsis; Ω , the ascending node; M , the mean anomaly.

Now borrow directly from the well-established theory of secular perturbations due to the J_2 oblateness term. Restating directly from Danby (equations 11.5.6), the secular rates of change are:

$$\frac{da_s}{dt} = 0 \quad (136)$$

$$\frac{dc_s}{dt} = 0 \quad (137)$$

$$\frac{di_s}{dt} = 0 \quad (138)$$

$$\frac{d\omega_s}{dt} = -\frac{3nJ_2}{2a^2(1-e^2)^{5/2}} \sin^2 i - 2 \quad (139)$$

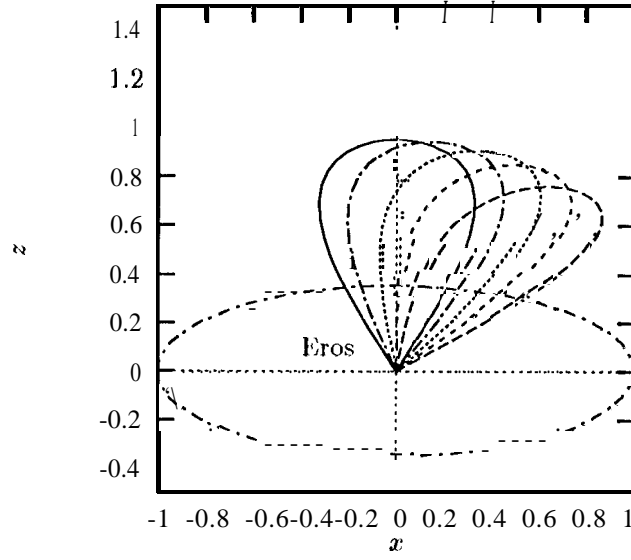


Figure 9: $x \times z$ Projection of Periodic Orbits

$$\frac{d\Omega_s}{dt} = -\frac{3nJ_2}{2a^2(1-e^2)^2} \cos i \quad (140)$$

$$\frac{dM_s}{dt} = n \left[1 - \frac{3J_2}{2a^2(1-e^2)^{3/2}} \left(\frac{3}{2} \sin^2 i - 1 \right) \right] \quad (141)$$

where $n = \sqrt{\mu/a^3}$. The subscript s denotes the secular part of the element.

These results match well with the stability results found for the direct orbits far from the ellipsoid and for the retrograde orbits about the ellipsoid. Further, comparisons between the above simple formulae and numerical integrations of satellite orbits about an ellipsoid show overall qualitative agreement, and close quantitative agreement for retrograde orbiters at inclinations below $\approx -25^\circ$.

A current research effort is being made which investigates satellite motion about an ellipsoid of revolution about its rotation axis. The results from this on-going analysis will have bearing on this current approximation and may allow for more precise results.

10.3 Numerical Results for Eros and Vesta

In concluding this section, representative nodal regression rates for a circular orbit at Eros and Vesta are presented. This is to indicate that the nodal regression rates that a satellite will face when orbiting an asteroid may be quite large, making the satellite orbit significantly non-Keplerian.

Assume that the satellite is in an orbit of inclination $i = -45^\circ$, eccentricity $e = 0$, and semi-major axis $a = 2\alpha$. Note that the inclination is negative, indicating a retrograde orbit.

10.3.1 Eros Characteristic Node Regression Rate

$$\frac{J_2}{\alpha^2} = 0.08775 \quad (142)$$

$$\mu = 8.79 \times 10^{-4} \text{ km}^3/\text{s}^2 \quad (143)$$

$$\dot{\Omega}_s = -13.5 \text{ deg/day} \quad (144)$$

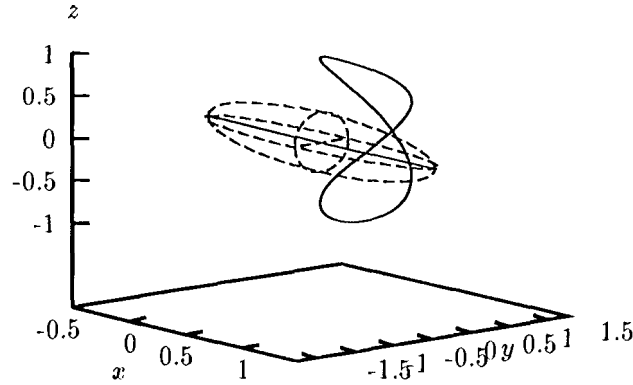


Figure 10: Three-Dimensional, Doubly-Symmetric Periodic Orbit

10.3.2 Vesta Characteristic Node Regression Rate

$$\frac{J_2}{\alpha^2} = 0.05116 \quad (145)$$

$$\mu = 14.257 \text{ km}^3/\text{s}^2 \quad (146)$$

$$\dot{\Omega}_s = -20.8 \text{ deg/day} \quad (147)$$

The above regression rates have been verified with numerical integration and are correct to the order of one degree/day. These results highlight, how even “stable” orbits about an asteroid may still be significantly non-K eplerian and have active dynamics in quantities such as the node and argument of the periaapsis. Note that the secular change in the argument of the periaapsis will be of the same order as the regression in the node in general].

11 Conclusion

The research described in this paper defines the problem of satellite dynamics about a tri-axial ellipsoid and arrives at some elementary results for this problem. All necessary formulae needed to compute the forces and partials for a satellite orbiting a tri-axial ellipsoid have been presented. The problem has also been non-dimensionalized and shown to depend on only three parameters; two shape parameters and one parameter relating the mass, size and rotation rate of the ellipsoid.

The zero-velocity surfaces of a satellite in orbit about the ellipsoid have been defined and described. All synchronous circular orbits about the ellipsoid were found as well as the conditions for their existence. The stability of these synchronous circular orbits were discussed and two classes of ellipsoids were defined according to whether any of the synchronous orbits were stable or not. Some specific computations of periodic orbit families were presented for two representative ellipsoids, based on actual asteroids. One of the orbit families discussed was three-dimensional, while the rest lay in the ellipsoid equator.

In the discussion, several items of interest were raised which merit further study. These items include further investigation of the periodic orbit families, analytic representation of the

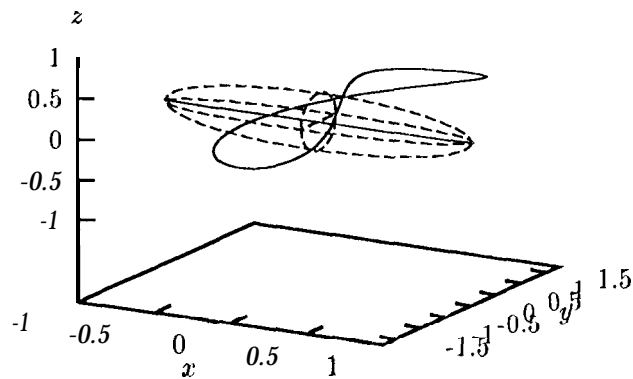


Figure 11: Three-Dimensional Periodic Orbit Intersecting the Ellipsoid

periodic orbits emanating from the equilibrium points, and improvements to the approximate theory of retrograde orbiters.

Acknowledgements

The research described in this paper was carried out by the Jet Propulsion Laboratory, California Institute of Technology, under contract with the National Aeronautics and Space Administration.

A Example Asteroids and Comets

Following is a table giving some of the known, measured physical characteristics of a few asteroids and comets. Note that the density values are not well known and are uncertain.

Name	Type	α (km)	β (km)	γ (km)	$2\pi/\omega$ (hours)	ρ (g/cc)	$\hat{\beta}$ (-)	γ (-)	$\&$	ρ_{\min} (g/cc)
Vesta	I	265	250	220	5.3	3.5	0.94	0.83	7.06	0.867
Eros	II	20	7	7	5.27	3.21	0.35	0.35	1.00	0.354
Gaspra	II	9.5	6	5.5	7	3.5	0.63	0.58	5.75	0.576
Iida	II	26	10.7	10.7	5	3.5	0.41	0.41	1.36	0.404
Tempel 2	II	8	4.25	4.25	8.95	1.0	0.53	0.53	2.07	0.508

B Computation of the Elliptic Integrals

The elliptic integrals defined by the ellipsoid potential function fall into forms that can be directly computed using published algorithms. First, recall the general form of the integral:

$$V = \frac{3}{4} \int_{\lambda}^{\infty} \frac{x^2}{\alpha^2 + u} + \frac{y^2}{\beta^2 + u} + \frac{z^2}{\gamma^2 + u} - 1$$

$$\frac{du}{\sqrt{(\alpha^2 + u)(\beta^2 + u)(\gamma^2 + u)}} \quad (148)$$

$$= \frac{3}{4} \int_0^\infty \left[\frac{x^2}{\alpha^2 + \lambda + u} + \frac{y^2}{\beta^2 + \lambda + u} + \frac{z^2}{\gamma^2 + \lambda + u} - 1 \right] \frac{du}{\sqrt{(\alpha^2 + \lambda + u)(\beta^2 + \lambda + u)(\gamma^2 + \lambda + u)}} \quad (149)$$

The Carlson form of the elliptic integrals used in our study are defined as:

$$R_F(\alpha^2, \beta^2, \gamma^2) = \frac{1}{2} \int_0^\infty \frac{du}{\sqrt{(\alpha^2 + u)(\beta^2 + u)(\gamma^2 + u)}} \quad (150)$$

$$R_D(\alpha^2, \beta^2, \gamma^2) = \frac{3}{2} \int_0^\infty \frac{du}{(\gamma^2 + u) \sqrt{(\alpha^2 + u)(\beta^2 + u)(\gamma^2 + u)}} \quad (151)$$

Note that the function R_F is symmetric in all its arguments, but that the function R_D is symmetric only in its first two arguments.

Using these forms, the potential may be written as:

$$V = \frac{1}{2} x^2 R_D(\beta^2 + \lambda, \gamma^2 + \lambda, \alpha^2 + \lambda) + \frac{1}{2} y^2 R_D(\gamma^2 + \lambda, \alpha^2 + \lambda, \beta^2 + \lambda) + \frac{1}{2} z^2 R_D(\alpha^2 + \lambda, \beta^2 + \lambda, \gamma^2 + \lambda) - \frac{3}{2} R_F(\alpha^2 + \lambda, \beta^2 + \lambda, \gamma^2 + \lambda) \quad (152)$$

Recalling that $\partial V / \partial \lambda \equiv 0$, the force partials are then:

$$V_x = x R_D(\beta^2 + \lambda, \gamma^2 + \lambda, \alpha^2 + \lambda) \quad (153)$$

$$V_y = y R_D(\gamma^2 + \lambda, \alpha^2 + \lambda, \beta^2 + \lambda) \quad (154)$$

$$V_z = z R_D(\alpha^2 + \lambda, \beta^2 + \lambda, \gamma^2 + \lambda) \quad (155)$$

Algorithms for computing the functions R_D and R_F are given in Reference [6], Section 6.11. The algorithms use a method similar to MacLaurin's Theorem to uniformly rescale the function arguments until they are approximately equal, at which point a Taylor series expansion may be introduced to explicitly solve for the value of the function.

B.1 A Special Identity

The identity stated in Equation 99 is derived here. This same identity is used elsewhere in the paper to simplify some of the stated results.

The identity is:

$$\frac{1}{\Delta(u)} = \frac{1}{2} \int_u^\infty \left[\frac{1}{\alpha^2 + u} + \frac{1}{\beta^2 + u} + \frac{1}{\gamma^2 + u} \right] \frac{du}{\Delta(u)} \quad (156)$$

$$A(u) = \sqrt{(\alpha^2 - u)(\beta^2 + u)(\gamma^2 + u)} \quad (157)$$

To prove this result, differentiate the quantity $1/A(u)$ with respect to the parameter u . This results in the equality:

$$\frac{d\Delta(u)^{-1}}{du} = -\frac{1}{2} \left[\frac{1}{\alpha^2 + u} + \frac{1}{\beta^2 + u} + \frac{1}{\gamma^2 + u} \right] \frac{1}{A(u)} \quad (158)$$

Now integrate the quantity over the parameter u from limits v to ∞ to find:

$$\int_v^\infty \frac{d\Delta(u)^{-1}}{du} du = -\frac{1}{2} \int_v^\infty du \left[\frac{1}{\alpha^2 + u} + \frac{1}{\beta^2 + u} + \frac{1}{\gamma^2 + u} \right] \frac{1}{A(u)} \quad (159)$$

The left hand side of the equation may be integrated exactly to yield:

$$\int_v^\infty \frac{d\Delta(u)^{-1}}{du} du = \frac{1}{\Delta(\infty)} - \frac{1}{A(v)} \quad (160)$$

$$= -\frac{1}{A(v)} \quad (161)$$

The identity then falls directly out of the results.

This identity is most useful in reducing the stability condition devaluated at the equilibrium points. In terms of the Carlson form of the elliptic integrals, this identity is stated as:

$$\frac{3}{\sqrt{(\alpha^2 + v)(\beta^2 + v)(\gamma^2 + v)}} = R_D(\beta^2 + v, \gamma^2 + v, \alpha^2 + v) + R_D(\gamma^2 + v, \alpha^2 + v, \beta^2 + v) + R_D(\alpha^2 + v, \beta^2 + v, \gamma^2 + v) \quad (162)$$

B.2 Reductions to Special Cases

Given in the paper are several results which rely on the evaluation of these elliptic integrals for some simplified cases, namely $\alpha = \beta$, $\beta = \gamma$ and $\alpha = \beta = \gamma$. In all these cases the elliptic integrals degenerate into quadrature which may be expressed in terms of elementary functions. The computation of the function R_D under all these special cases are listed below.

B.2.1 $\alpha = \beta = \gamma$

$$R_D(\alpha^2 + \lambda, \alpha^2 + \lambda, \alpha^2 + \lambda) = \frac{3}{2} \int_0^\infty \frac{du}{(\alpha^2 + \lambda + u)^{5/2}} \quad (163)$$

$$= \frac{1}{\alpha^2 + \lambda} \quad (164)$$

B.2.2 $\alpha > \beta = \gamma$

$$R_D(\alpha^2 + \lambda, \beta^2 + \lambda, \beta^2 + \lambda) = \frac{3}{2} \int_0^\infty \frac{du}{(\beta^2 + \lambda + u)^2 \sqrt{\alpha^2 + \lambda + u}} \quad (165)$$

$$= \frac{3\sqrt{\alpha^2 + \lambda}}{2(\alpha^2 - \beta^2)(\beta^2 + \lambda)} - \frac{3}{4(\alpha^2 - \beta^2)^{3/2}} \ln \frac{1 + \sqrt{\frac{\alpha^2 - \beta^2}{\alpha^2 + \lambda}}}{1 - \sqrt{\frac{\alpha^2 - \beta^2}{\alpha^2 + \lambda}}} \quad (166)$$

$$R_D(\beta^2 + \lambda, \beta^2 + \lambda, \alpha^2 + \lambda) = \frac{3}{2} \int_0^\infty \frac{du}{(\beta^2 + \lambda + u)(\alpha^2 + \lambda + u)^{3/2}} \quad (167)$$

$$= \frac{-3}{(\alpha^2 - \beta^2)\sqrt{\alpha^2 + \lambda}} + \frac{3}{2(\alpha^2 - \beta^2)^{3/2}} \ln \frac{1 + \sqrt{\frac{\alpha^2 - \beta^2}{\alpha^2 + \lambda}}}{1 - \sqrt{\frac{\alpha^2 - \beta^2}{\alpha^2 + \lambda}}} \quad (168)$$

B.2.3 $\alpha = \beta > \gamma$

$$R_D(\alpha^2 + \lambda, \alpha^2 + \lambda, \gamma^2 + \lambda) = \frac{3}{2} \int_0^\infty \frac{du}{(\alpha^2 + \lambda + u)(\gamma^2 + \lambda + u)^{3/2}} \quad (169)$$

$$= \frac{2}{(\alpha^2 - \gamma^2)\sqrt{\gamma^2 + \lambda}} - \frac{2}{(\alpha^2 - \gamma^2)^{3/2}} \arctan \sqrt{\frac{\alpha^2 - \gamma^2}{\gamma^2 + \lambda}} \quad (170)$$

$$R_D(\alpha^2 + \lambda, \gamma^2 + \lambda, \alpha^2 + \lambda) = \frac{3}{2} \int_0^\infty \frac{du}{(\alpha^2 + \lambda + u)^2 \sqrt{\gamma^2 + \lambda + u}} \quad (171)$$

$$= -\frac{3\sqrt{\gamma^2 + \lambda}}{2(\alpha^2 - \gamma^2)(\alpha^2 + \lambda)} + \frac{3}{2(\alpha^2 - \gamma^2)^{3/2}} \arctan \sqrt{\frac{\alpha^2 - \gamma^2}{\gamma^2 + \lambda}} \quad (172)$$

References

- [1] M. Hénon, "Exploration Numérique du Problème Restreint. II.", *Annales D'Astrophysique*, Vol 28, No 6, pp 992-1007, 1965.
- [2] M. Hénon, "Numerical Exploration of the Restricted Problem. V.", *Astronomy and Astrophysics*, Vol 1, pp 223-238, 1969.
- [3] M. Hénon, "Numerical Exploration of the Restricted Problem. VI.", *Astronomy and Astrophysics*, Vol 9, pp 24-36, 1976.
- [4] W.D. MacMillan, The Theory of the Potential, Elsevier, 1930.
- [5] C. Marchal, The Three-Body Problem, McGraw-Hill, 1990.
- [6] W.H. Press, et. al., Numerical Recipes in Fortran, 2nd Ed., Cambridge University Press, 1992.
- [7] D.J. Scheeres, On Symmetric Central Configurations with Application to Satellite Motion About Rings, Doctoral Dissertation, The University of Michigan, 1992.